Design and Development of low-cost Sensor to capture ventral and dorsal Finger-vein for Biometric Authentication

Raghavendra Ramachandra, Kiran Raja, Sushma Venkatesh and Christoph Busch

***Abstract*—Biometrics-based authentication of subjects is widely deployed in several real-life applications. Among various biometric characteristics, finger-vein characteristic has demonstrated both reliable and highly accurate authentication for access control in secured applications. However, most of these systems are based on commercial sensors where the image level data is not available for academic research. In this paper, we present the design and development of a low-cost finger-vein sensor based on a single camera that can capture finger-vein images from dorsal and ventral part of the finger with high quality. The system consists of multiple Near-Infra-Red (NIR) light sources to illuminate the finger from both sides (left and right) and top. The camera in the sensor is also coupled with the custom designed physical structure to facilitate high reflectance of the emitted light and distribute the light uniformly on the finger to capture good quality dorsal and ventral finger-vein pattern. Extensive experiments are carried out on the data captured using the developed sensor and benchmarked the performance with eight different State-Of-The-Art (SOTA) algorithms. The results on a large-scale finger-vein dataset demonstrate the need for illumination from both sides (left and right) and from the top of the finger, to capture finger-vein images with high quality that improves the verification performance.**

***Index Terms*—Biometrics, finger-vein sensor, dorsal finger-vein, ventral finger-vein, sensor.**

I. Introduction

The increased demand for reliable and accurate authentication in secure applications has led to an interest in employing the finger vascular pattern (aka., finger-vein) as a biometric modality. Finger-vein biometrics are known to deliver high verification accuracy and this has boosted the adaptability of finger-vein biometrics in the finance sectors for secure banking transactions and other high secure applications. The finger-vein system is primarily based on extracting the structure of the vascular pattern in the finger which are visible in the NIR light only. As finger-vein patterns are present beneath the skin, they are neither susceptible to abrasion nor to changes in the surface of the skin (e.g. for cuts or abrasions) making them robust against presentation attacks (a.k.a. spoofing attacks). Even when attacked on finger-vein sensors through presentation attacks/spoofing attacks, they can be detected easily by analyzing the different spatial and temporal differences [1].

The underlying principle in designing a finger-vein sensor is by illuminating a finger with NIR light which is absorbed in higher proportion by Haemoglobin than the neighboring tissues resulting in highlighted vein pattern within the finger. The use and arrangement of the light source to illuminate the finger plays a vital role in extracting a good quality finger-vein pattern. The conventional arrangements in the finger-vein sensor can be broadly classified to have two types such as [2]: (a) Light penetration approach (b) Light reflection approach. Most of the current day finger-vein sensors are based on the penetration approach that can provide a good quality finger-vein image when compared to the reflection approach. The light penetration approaches can be further divided in two types: (a) Top-illuminated - illumination from the top of the finger (b) Side-illuminated - illumination from the side (both left and right side) of the finger.

In the case of a top-light illuminated sensor, the Light-Emitting-Diode (LED) is placed above the finger and the camera is placed below the finger. The light emitted from the LEDs is penetrating through the finger and is absorbed by the vein patterns due to the presence of haemoglobin. This makes the vein region appear darker than the neighborhood tissues when recorded by the camera, resulting in the capture of a finger-vein pattern. The NIR wavelength of 850nm is widely used to illuminate the finger.

With side-light illuminated sensors, the LED lights are placed on both sides of the finger and illuminated simultaneously. The camera is placed below the finger that captures the vein image. Despite the side-illumination using a higher number of LEDs (at 850nm) to achieve uniform illumination of the finger surface, the quality of the finger-vein image has been reported to be better with light penetration approaches [3].

Earlier works on finger-vein sensors and capture devices were carried out by the industrial stakeholders Hitachi, Mofria and IDEMIA that have explored both side and top light illumination. Figure 1 shows examples of commercial finger-vein sensors and Table I presents the properties of such sensors, especially in terms of the hardware and the components employed to design the same. The common features across all commercial finger-vein sensors are on the use of NIR spectra to capture the finger-vein images. Depending on the design and placement of the finger one can easily locate the type of illumination (top or side). The common information that was made available from finger-vein vendors are the performance metrics that include False Acceptance Rate (FAR), False Reject Rate (FRR) and Failure To Enrol (FTE). It is also interesting to note that all commercial sensors

R.Raghavendra, K.Raja, S.Venkatesh and C. Busch are with the Norwegian Biometrics Laboratory, Norwegian University of Science and Technology (NTNU), Gjøvik, Norway e-mail: (raghavendra.ramachandra, kiran.raja,sushma.venkatesh,christoph.busch) @ ntnu.no

Fig. 1: Examples of commercial sensors (a) MOFRIA (b) EKEMP (c) BARCLAYS (d) IDEMIA (e) HITACHI (f) M2SYS (g) SONY

Company	Camera and Lens	Accuracy	Type of illumination
EKEMP	No information	FRR = 0.01%, FAR = 0.00001% FTE = 0.001%	Top illumination
M2SYS	NIR camera	FRR = 0.01%, FAR = 0.0001%, FTE = 0%	Top illumination
HITACHI	No information	FRR = 0.01%, FAR = 0.0001%, FTE = 0.03%	Side illumination
Barclays	No information	No information	No information
IDEMIA	No information	FRR = no information , FAR = 0.0001%, FTE = 0%	Side illumination
KO-Vein	No information	FRR = 0.01%, FAR = 0.0001%, FTE = 0.%	Side illumination
MOFIRIA	No information	No information	Side illumination

TABLE I: Characteristics of commercial finger-vein sensor

are compact, fast transaction times (in terms of a millisecond to authenticate the single query), good storage capabilities (to store 2000 to 5000 finger-vein template) and are powered through USB. However, the detailed hardware description is not available for commercial finger-vein sensors. Further, none of the commercial sensors provides access to the captured raw finger-vein images neither to the templates as these are encoded in a proprietary format, further protected by the manufacturer. In addition to these commercial sensors, there also exists an academic sensor from EKEMP. However, the technical details, especially in terms of component-hardware and access to the raw finger-vein images, are not available.

During recent years, the academic versions of finger-vein sensors have emerged with different design and specification to improve the finger-vein image quality and thereby improve the performance of authentication. Figure 2 illustrates the academic finger-vein devices and Table II indicates the characteristics of the academic finger-vein sensors. The majority of the academic sensors measure larger than commercial sensors that can be attributed to the modular design adopted by academic researchers. The interesting characteristics of all these sensors are: (a) All sensors have used the NIR camera with a filter (NIR/IR pass) and a lens. The camera quality

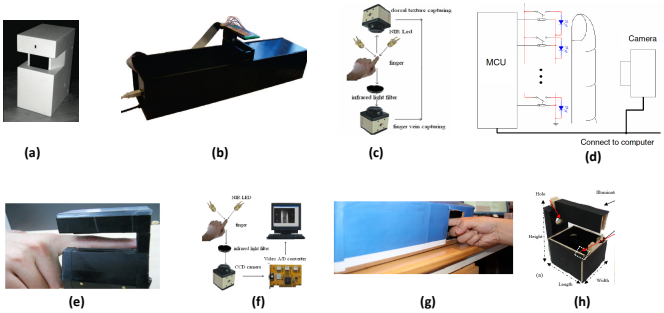

Fig. 2: Examples of commercial sensors (a) Hung et al. [4] (b) B. H Ton et al. [5] (c) W. Tang et al. [6] (d) X. Xi [7] (e) W. Yang [8] (f) R. Raghavendra et al. [9] (g) Y. Lu et al. [10] (h) T. D. Pham et al. [11]

is also varied across different sensors from the expensive industrial cameras [5] to low-cost web camera [11]. (b) A different spectral wavelength within NIR band is used for the illumination. Thus, the spectral wavelength is varied from 850nm till 940nm. (c) The majority of the sensors have used the top-light illumination and very few have used the side-light illumination. However, as noted from the commercial sensors (see Table I) the majority of them are based on the side-light illumination. Thus, the position of the illumination (top/side) is based on the finger placement that can impact the user experience. (d) Even though most of the academic sensors have provided the information on the sensor components none of them discussed the design aspect and also the more technical aspects of the light source, for example, type of the LEDs and the view angle. This will limit one to successfully reconstruct the finger-vein sensor.

Authors	Camera and Lens	Capture Wavelength	Type of illumination
Hung et al. [4]	1/3 inch CMOS camera	No information	Top illumination
B. H Ton et al. [5]	Pentax H1214-M /IR cut filter	850nm	Top illumination
W. Tang et al. [6]	No information	890nm	Top illumination
T. Dai et al. [12]	172 inch CCH (SV1310FM, Da-heng Optics)	No information	Top illumination
M. Kono et al. [13]	NIR CCD camera	No information	Top illumination
X. Xi [7]	No information	No information	Top illumination
J. kim et al. [14]	CCD camera (GF 038B NIR)	850nm	Top illumination
W. Yang [8]	No information	850nm	Top illumination
R. Raghavendra et al. [9]	DMK 22BUC03 CMOS / 8mm	870nm	Top illumination
Y. Lu et al. [10]	NIR camera	850nm	Top illumination
H. dana [15]	No information	900nm	Side illumination
T. D. Pham [11]	Webcamera	850nm	Top illumination

TABLE II: Characteristics of academic finger-vein sensor

Although reasonable efforts have been made in developing finger-vein sensors, it is still difficult to prefer a type of illu-

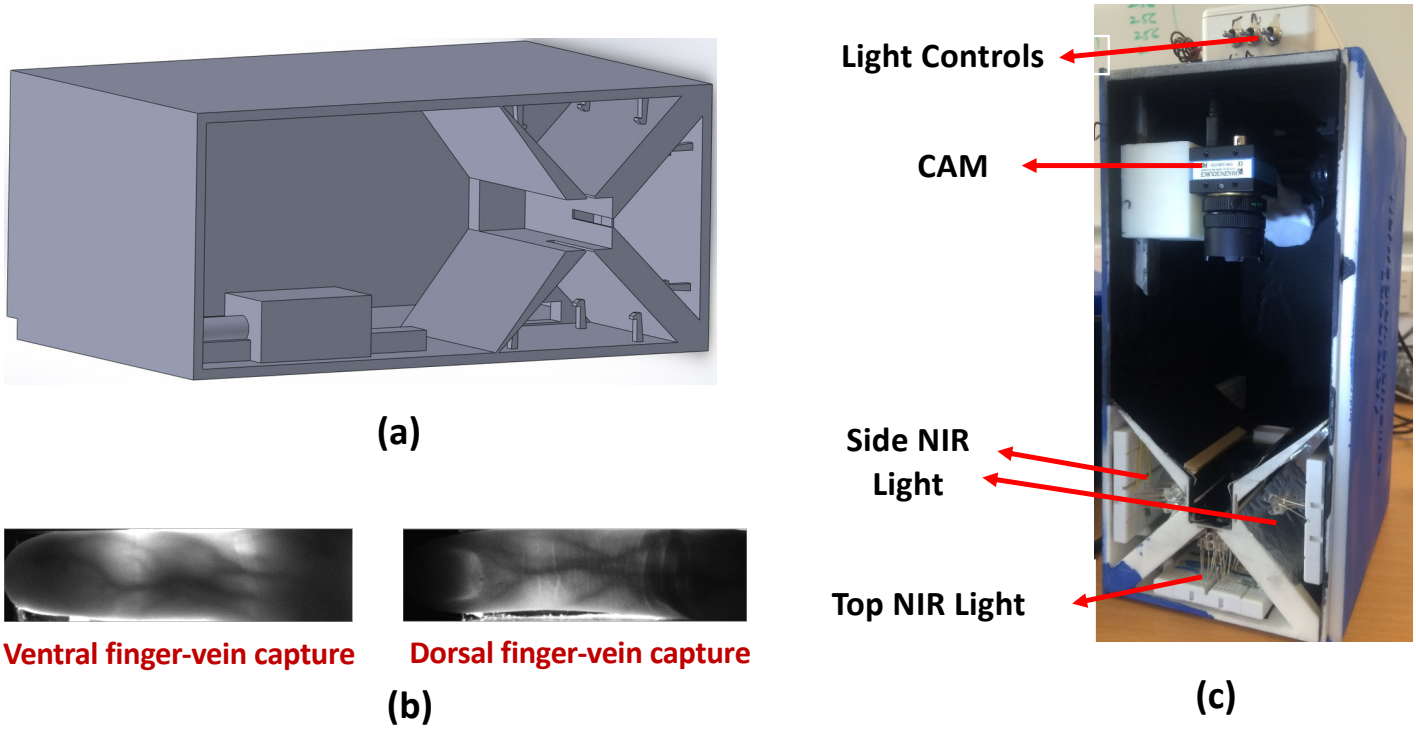

Fig. 3: Developed finger-vein sensor with captured dorsal and ventral finger-vein images (a) Sensor design layout (b) Captured finger-vein images (c) Sensor components

mination (top/side) and a kind of finger-vein capture concept (dorsal/ventral), which improves both reliability and accuracy of the finger-vein verification. Therefore, in this paper, we aim to answer the following questions:

Q1: What type of light illumination (top or side) contributes effectively to improve the finger-vein verification performance?
Q2: Does the use of illumination from both top and side improve the finger-vein verification performance?
Q3: What kind of finger-vein capture concept (dorsal/ventral) can provide better performance on the large-scale finger-vein database?

To the best of our knowledge, this is the first work that empirically presents the answers to the above research questions.

To effectively answer these questions, it is essential to collect a new finger-vein database with three different light illumination such as the top, side and both (in which both side and the top finger is illuminated). Further, it is also essential to collect a new database with dorsal and ventral finger-vein patterns corresponding to the same finger instance with the same capturing conditions and the sensor. These factors motivated us to design and develop a low-cost finger-vein capture device. The proposed finger-vein sensor thus has a unique design that can accommodate the illumination from both sides and top of the finger. The sensor further houses a physical structure to focus the illumination that enables the high-quality imaging of the finger-vein biometrics. Further, the design aspects are focused on accommodating the pleasant user experience while capturing both dorsal and ventral finger-vein images in two different instances.

The main contributions of this paper are:

- Design and development of a low-cost finger-vein sensor that can capture both ventral and dorsal finger-vein pattern in two different representations and three different illuminations on the finger such as top, side and both (top and side). The design details are provided such that an interested researcher can re-build such a sensor without spending time for component selection and design.
- New finger-vein database comprised of 350 different finger-vein (both ventral and dorsal) samples, captured in three different illuminations referred to as top, side and both. We refer this database as DB-I in the rest of the paper.
- New large-scale finger-vein database comprised of 1084 unique finger-vein samples using both illuminations to provide the comparative analysis of dorsal and ventral finger-vein patterns. We refer to this database as DB-II in the rest of the paper.
- Extensive experiments with eight different state-of-the-art finger-vein verification methods on both DB-I and DB-II databases.

The rest of the paper is organised as follows: Section II presents the design and development of our low-cost finger-vein sensor, Section III presents the state-of-the-art finger-vein verification systems, Section IV presents the details of the data collection enabled by the developed finger-vein sensor, Section V presents the experimental results and discussion. Section VI provides the conclusion and remarks of this work.

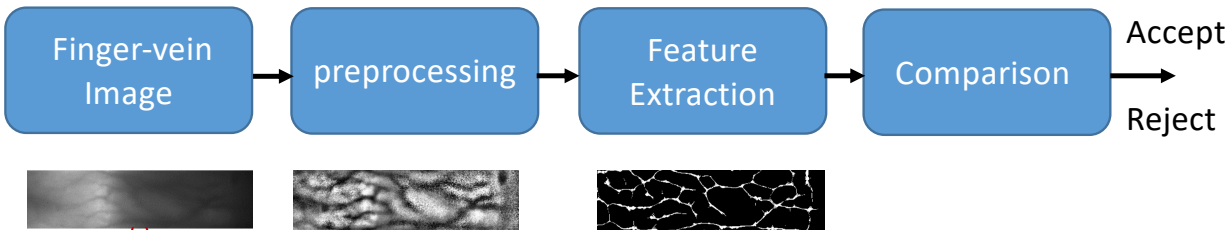

Fig. 4: Block diagram of finger-vein verification system

Fig. 5: Illustration of a finger-vein sample captured with different illuminations

II. Developed finger-vein sensor

Figure 3 illustrates the developed sensor design and the associated components. The developed sensor has three integral parts (1) NIR Camera (2) NIR light source (3) Dedicated (customized) physical structures to achieve high radiance of the illuminated light. We employed the NIR camera *DMK 22BUC03 monochrome CMOS* with a resolution of 744×480 pixel that has good quantum efficiency in NIR spectral band. The camera has been equipped with *T3Z0312CS* lens with a focal length of $8mm$. The NIR lighting source is based on three independent LED clusters that emit an adequate amount of light to capture the finger-vein pattern. The first two NIR LED clusters are developed using a cluster of 10 LEDs (for side illumination) and third LED cluster (top illumination) is comprised of 40 LEDs. We have employed NIR LEDs *TSFF 5210* with a wavelength of $920nm$ by considering it's high radiant intensity and view angle that results in good illumination on a finger.

The key part of the sensor is the custom designed physical structure that enables adequate intensity of lighting to penetrate into the finger to achieve a good quality of the finger-vein image. Two different physical structures are developed, the first structure is designed to concentrate the emitted light intensity to the small area. The walls of the first structure are coated using a reflective aluminum foil to increase the radiance of the light further. The second physical structure is designed to act as a single slit such that the non-uniform light crossing this slit becomes uniform [16].

The sensor is constructed by considering the ergonomic convenience such that the user can place the finger (irrespective of size and shape) without any difficulty/pressure on the finger. This is achieved by introducing a holder that allows the finger to be easily rested and also restricts the involuntary movement of the fingers to get the stable and consistent finger-vein image without any blur factor introduced by minor motion. Figure 5 shows the example finger-vein image captured using the proposed sensor in three different types of illumination.

III. Baseline finger-vein verification

Fig. 4 shows the block diagram of the finger-vein verification system employed in this work. The main objective of this work is to quantify the finger-vein verification performance across different kinds of light illumination that are widely used in designing the finger-vein capture device. To this extent, we have employed eight different well know finger-vein verification systems as the baseline methods.

The finger-vein biometrics is well addressed by the researchers that have resulted in numerous features extraction and comparison techniques. The systematic survey of finger-vein feature extraction techniques is presented in [17]. The available feature extraction techniques can be widely divided in two types namely: Local features and global features. The local features extract the features pertaining to the finger-vein structure that includes the line patterns and the minutia points. The main advantage of the local features is the use of simplified comparators like non-cumulative template comparison algorithm or a simple distance measures (binary). Further, the local feature based methods have indicated robust accuracy, also computationally efficient and well suited to work with a single enrolment sample as the comparators are based on non-learning techniques. The global feature methods extract either image gradients or the texture based information from the finger-vein images. The comparator corresponding to the global features are normally based on the machine learning techniques and thus, need more image samples per subject to train the same to achieve the desired accuracy.

In this work, we evaluate both local and global features that are widely used in the finger-vein literature by considering their performance accuracy. The local feature extraction methods employed in this work include: Maximum Curvature Pattern (MCP) [18], Spectral Minutiae Representation (SMR) [19] and Repeated Line Tracking (RLT) method [20]. We have used the non-cumulative template comparison algorithm [18] as the comparator for all three local feature extraction techniques to quantify the performance. Further, we have also employed four different global feature extraction techniques that include:

LBP features [21], LBPV features [22], Steerable features [23] and HoG features [24]. As it is well demonstrated in the literature that the use of machine learning based comparator has demonstrated the best performance with global features, in this work, we have employed Probabilistic Collaborative Representation Classifier (P-CRC) [25] [26] by considering its accuracy and less computational cost. Thus, the use of the same comparator on different global features allows one to quantify the performance of the different global features for finger-vein verification. We also note the recent advances in the machine learning made it possible to employ an end-to-end finger-vein system using a deep learning approach based on the Convolutional Neural Network (CNN) [27] that have indicated a reliable performance of the finger-vein verification system. We have therefore evaluated an end-to-end finger-vein algorithm using deep CNN architecture [27]. For a more detailed description of the feature extraction and comparator techniques, readers are referred to the above-mentioned respective references. All these eight different finger-vein algorithms are evaluated independently on both DB-I and DB-II databases.

IV. Finger-vein Database collection

We have used the newly developed finger-vein sensor to collect two different databases that in turn allowed us to test and benchmark the applicability of the developed sensor in real-life applications. In this work, we have collected two different databases referred as DB-I and DB-II. The first database (DB-I) is collected to evaluate the performance of the finger-vein (Dorsal and Ventral) patterns with three different light illuminations positions such as (a) *from the Side* (b) *from the Top* (c) *Both - side and top*. The DB-I is comprised of 350 individual finger-vein samples collected in 10 different sessions (over a duration of 1 - 15 days) that has resulted in $350 \times 10 = 3500$ ventral and dorsal finger-vein samples correspondingly. The performance of four different SOTA algorithms is reported by following the evaluation protocol with 9 samples as the enrolment sample and 1 sample as the probe for each unique finger-vein instance. Thus, for each trial, we have $350 \times 1 = 350$ genuine scores and $350 \times 349 \times 1 = 122150$ impostors scores. We repeat the selection of reference and probe samples ten times and the average of the results are reported together with the 90% Confidence Interval (CI) in terms of Genuine Match Rate (GMR) @ False Match Rate (FMR) of 10^{-3}. Figure 5 illustrates the example finger-vein (ventral) that is captured in three different light illumination conditions. It is interesting to observe that the perceptual quality of the finger-vein image is better when both side and top illumination on the finger is used.

The second database (DB-II) is collected using *Both* illumination to quantify the performance of the ventral versus dorsal finger-vein samples. DB-II is comprised of 1084 unique finger-vein (both ventral and dorsal) samples collected in 10 different sessions (in the duration of 1 - 15 days) which has resulted in database with $1084 \times 10 = 10840$ ventral finger-vein samples and $1084 \times 10 = 10840$ dorsal finger-vein samples. To evaluate the performance on DB-II, we divided the whole database to have a development dataset (only to tune the parameters of SOTA) of 100 unique finger-vein instances and the remaining 984 unique instances are used to report the results. We follow the same evaluation protocol of DB-I with 9 samples used as enrolment and 1 sample as a probe that results in 984 genuine scores and 967272 impostors scores. Finally, the selection of enrolment and probe samples are repeated 10 times and the average results with the 90% CI are reported. Figure 3 (b) illustrates the example of the dorsal and ventral finger-vein samples that are captured using the developed finger-vein sensor. *The database is available semi-publicly for research purpose upon the request to authors.*

V. Experiment and results

In this section, we present the quantitative experimental results on both DB-I and DB-II databases. The performance reported in this paper is based on the definitions of International Standard ISO/IEC 19795-1:2006 on Biometric Performance Testing and Reporting (BPTR) [28]. Thus, the results are presented using the ROC curves with FMR and FNMR.

The ROC curves describe the relationship between FMR and GMR = 1- FNMR that are established through the accumulation of the ordered genuine and impostor scores [28]. Since the ROC curves are plotted with FMR versus GMR = 1- FNMR, it will allow one to quickly verify the performance of the biometric system by setting the decision threshold at a particular FMR.

We have performed two different experiments (1) **Experiment 1:** Presents the performance of the SOTA finger-vein algorithms on three different kinds of illumination independently on the medium sized database of 350 unique finger-vein instances (DB-I). Thus, this experiment will provide a quantitative analysis of what type of illumination can improve the overall performance of the finger-vein biometrics. In this experiment, results are reported independently on dorsal and ventral finger-vein patterns. This experiment is designed to answer the question Q1 and Q2. (2) **Experiment 2:** This experiment is designed to compare the performance of the dorsal finger-vein with ventral finger-vein patterns that are collected with both (side and top) illumination. This experiment will use the DB-II database to report the results independently on dorsal and ventral finger-vein patterns. This experiment is designed to answer the question Q3.

A. Experiment 1: Results and discussion

Table III shows the performance of eight different state-of-the-art techniques that includes both local and global feature extractions schemes together with deep CNN technique. The comparison scores for the local features are obtained using the non-cumulative template comparison algorithm mentioned in [18] and comparison scores for the global feature extraction schemes are obtained using Probabilistic Collaborative Representation Classifier (P-CRC). Figure 6 and 7 indicates the receiver operating curves corresponding to eight different finger-vein verification system on dorsal and ventral finger-vein pattern respectively.

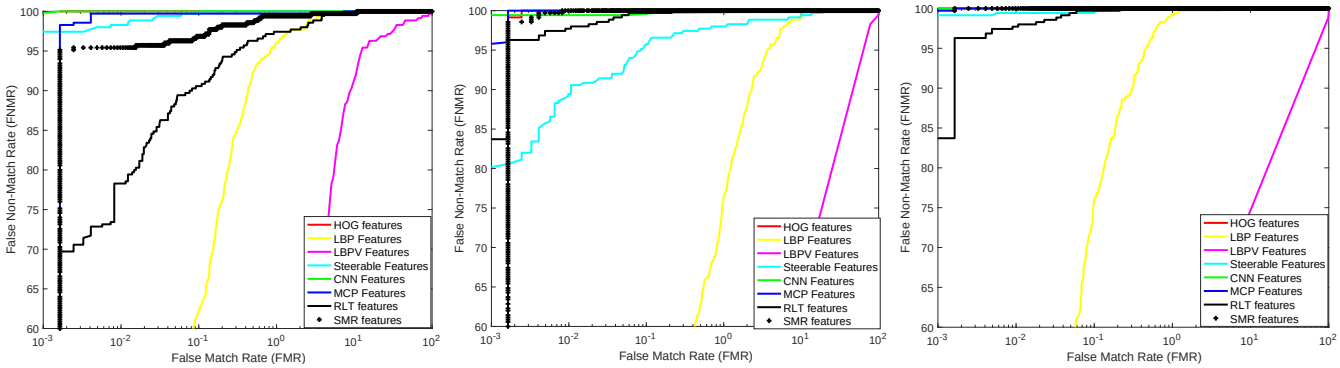

(a) Side Illumination (b) Top Illumination (c) Both Illuminations

Fig. 6: Performance of Dorsal finger-vein with Side, Top and Both Illuminations

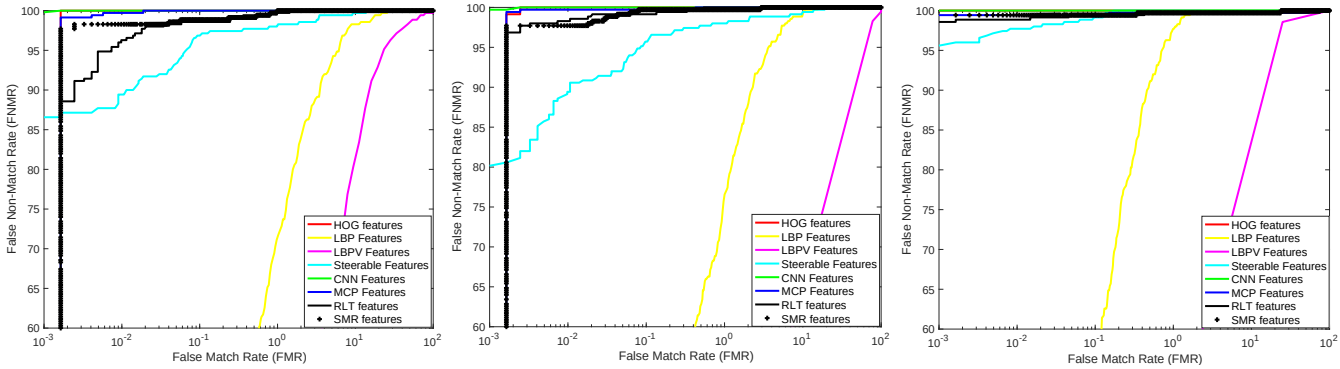

(a) Side Illumination (b) Top Illumination (c) Both Illuminations

Fig. 7: Performance of Ventral finger-vein with Side, Top and Both Illuminations

Algorithms		Side illumination		Top illumination		**Both illuminations**	
		GMR @ FMR = 10^{-3} ± CI		GMR @ FMR = 10^{-3} ± CI		GMR @ FMR = 10^{-3} ± CI	
		Dorsal	Ventral	Dorsal	Ventral	Dorsal	Ventral
Global features	HoG features [24]	99.43 ± 0.18	96.85 ± 0.02	100 ± 0	100 ± 0	**100 ± 0**	**100 ± 0**
	LBP features [21]	2.28 ± 0.11	5.71 ± 0.15	4.57 ± 0.19	4.57 ± 2.14	**6.75 ± 0.15**	**8.56 ± 1.96**
	LBPV features [22]	0 ± 0	0 ± 0	0 ± 0	0 ± 0	**0 ± 0**	**0 ± 0**
	Steerable features [23]	97.43 ± 0.87	86.57 ± 0.14	80.57 ±0.43	80.67 ± 0.56	**100 ± 0**	**96.78 ± 0.01**
	CNN [27]	99.72 ± 0.41	97.71 ± 0.34	99.43 ± 0.41	98.78 ± 0.01	**100 ± 0.02**	**100 ± 0**
Local features	MCP [18]	9.42 ± 0.24	19.14 ± 0.01	96.12 ± 0.0	24.41 ± 0.24	**99.71 ± 0**	**98.57 ± 0.24**
	SMR [19]	7.42 ± 0.35	16.85 ± 0.34	47.42 ± 0.0	24.28 ± 0.24	**99.71 ± 0**	**99.42 ± 0.25**
	RLT [20]	25.42 ± 0.64	2.10 ± 0.34	83.71 ± 0.24	19.71 ± 0.24	**97.71 ± 0**	**98.57 ± 0.25**

TABLE III: Performance of the SOTA finger-vein recognition algorithms on different kind of illuminations

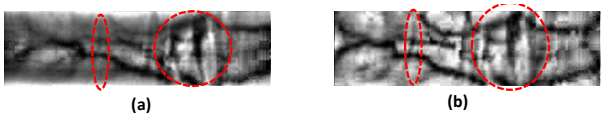

Fig. 8: Illustration of the dorsal finger-vein sample captured with different illuminations indicating the finger knuckle features (marked in red circles) (a) side-light illumination (b) top-light illumination

Based on the obtained results for both Dorsal (see Figure 6 and Table III) and Ventral (see Figure 7 and Table III), the following points can be noted:

- The performance of the finger-vein verification with local features especially with side-light illumination has resulted in degraded performance (when compared to that of top-light and both-light illumination) on both ventral and dorsal finger-vein patterns. A similar observation is also noted with the texture based global features. The possible reason for the degraded performance can be attributed to the way the light is illuminated on the finger. With the use of the side-light illumination process illuminating the light on both sides of the fingers, the chances are that the illumination process is blocked by the distal phalanx of the finger. This results in low-quality image capture outcomes, where the finger-vein pattern (in both ventral and dorsal) is less visible. This fact can be justified from the Figure 5 in which the side illumination shows the poor quality of finger-vein patterns. As the local features are based on extracting the vein patterns and then locating the minutia points, there are many changes that these features are not effectively extracted due to the insufficient light illumination. Further, the degradation of the texture based approaches can be attributed to the lack of texture information in finger-vein images captured in the NIR spectrum.
- It is interesting to observe the outstanding verification performance of the global features based on HoG and the CNN based approaches on the side light illumination. The accurate performance of the HoG features can be attributed to the robustness of HoG to the rotation and illumination. Along the same lines, the CNN based approach can learn the robust features from the data and thus result in the accurate performance.
- The performance of the finger-vein verification based on both local and global features are greatly improved with top-light illumination. However, the texture based global features based on LBP and LBPV have indicated the degrading performance and can be attributed to the lack of texture information as images are captured in the NIR spectrum. Further, it is also noted that the performance of the local feature based on SMR has indicated the degraded performance when compared to that of the other two different local feature methods. Since the SMR method is based on the minutiae extraction, adequate illumination is required to accurately locate the same. Thus, the lack of illumination has resulted in the degraded performance of the SMR method.
- Even with the top-light illumination, both HoG and CNN based approach have indicated an outstanding performance. This fact further justifies the robustness of both of these methods to the type of light illumination (side or top).
- It is interesting to observe that local features based techniques especially based on MCP features have indicated the good performance on the dorsal finger-vein pattern when compared with the ventral finger-vein pattern. After carefully observing the dorsal finger-vein images captured with top light illumination, it can be attributed to the type of illumination in which the dorsal finger-vein is captured together with the residues of the finger knuckle. This will result in line features when MCP is used, as the residues of finger knuckles are unique for each finger, this has contributed to the increased performance. Figure 8 illustrates the presence of finger knuckle features together with the dorsal finger-vein pattern.
- With both-light illumination, the performance of the SOTA algorithms on both dorsal and ventral finger-vein are drastically improved. This fact justifies the use of both (side and top) illumination together with the physical structures to capture the high-quality finger-vein imaging. However, the texture based method has resulted in a degraded performance, which is due to the lack of texture information as images are captured in the NIR spectrum.
- The performance of the dorsal and ventral finger-vein, especially with both-light illumination has indicated similar verification performance.
- Based on the extensive experiments, it is evident that the use of both-light illuminations has resulted in significant improvement in the accuracy irrespective of the finger-vein verification algorithms employed in this work. The improved accuracy is attributed to the larger visibility of the finger-vein pattern that contributes to the effective feature representations useful to improve the verification accuracy. It is also observed that the performance of local features are highly dependent on the type of the light illumination and it is well demonstrated that the use of both-light illuminations can significantly improve the performance.
- The best performance is note with both HoG and CNN with GMR = 100% @ FAR = 10^{-3} with both light illumination justifies the quality of the finger-vein images and it's application to the real-world scenario.

B. Experiment 2: Results and discussion

Figure 9 shows the Receiver Operating Characteristic (ROC) curve obtained on DB-II on both ventral and dorsal finger-vein patterns. Table IV indicates the quantitative performance of the eight different state-of-the-art finger-vein verification algorithms on both ventral and dorsal finger-vein patterns. In this experiment, the data is captured using both (side and top) illumination and thus, the good quality finger-vein samples are employed. The following are main observations from this experiment:

- Majority of the state-of-the-art finger-vein verification algorithms have demonstrated a reasonable verification

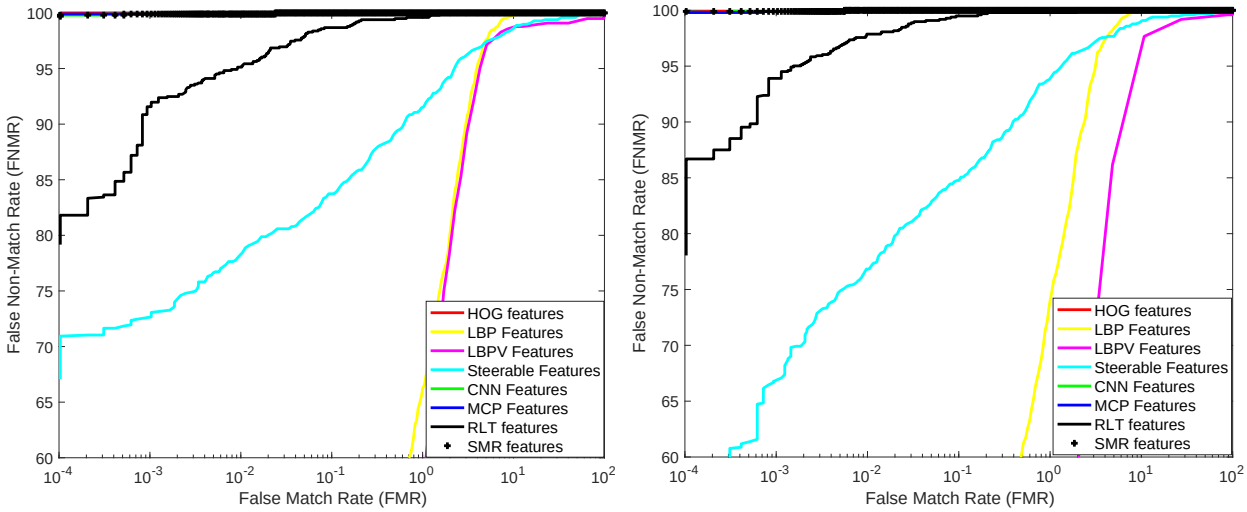

Fig. 9: Verification performance and ROC curves on DB-II (a) Dorsal finger-vein (b) Ventral finger-vein

Algorithms		GMR @ FMR = 10^{-4} ± CI	
		Dorsal Fingervein	Ventral Fingervein
Global Features	HoG features [24]	99.91 ± 0.25	99.97 ± 0.18
	LBP features [21]	0 ± 0	1.93 ± 0.78
	LBPV features [22]	0 ± 0	0 ± 0
	Steerable features [23]	68.39 ± 0.45	53.46 ± 0.89
	CNN [27]	99.85 ± 0.03	99.82 ± 0.28
Local features	MCP [18]	99.84±0.25	99.73 ± 0.75
	SMR [19]	99.89 ± 0.39	99.93 ± 0.65
	RLT [20]	78.36 ± 5.09	82.37 ± 0.18

TABLE IV: Performance of the SOTA finger-vein recognition algorithms on DB-II

accuracy on both ventral and dorsal finger-vein.

- Along the same lines of earlier observation, the texture based features resulted in a degraded verification performance that can be attributed to the lack of texture information as images are captured in the NIR spectrum.
- All three different local feature based finger-vein verification algorithms have demonstrated high performance on both ventral and dorsal finger-vein patterns. This can be attributed to the type of light illumination i.e, both-light illumination employed to collect the DB-II.
- Among the global feature-based approaches the HoG and CNN based features have demonstrated the outstanding performance. The HoG features has indicated a performance of GMR = 99.91%@FMR= 10^{-4} and GMR = 99.97%@FMR= 10^{-4} on dorsal and ventral finger-vein patterns respectively. The similar performance is also noted with the CNN based approach.
- Both ventral and dorsal finger-vein patterns have indicated a similar performance with three different state-of-the-art finger-vein verification algorithms. This justifies the applicability of the dorsal finger-vein patterns as a potential biometric characteristic together with the ventral finger-vein.

Based on the obtained results following are the precise answers for the research questions addressed in this work:

Q1: The use of top-light illumination has resulted in an improved performance on both dorsal and ventral finger-vein verification.

Q2: It is very evident that the use of both-light illuminations has significantly improved the performance of finger-vein verification algorithms.

Q3: With both-light illumination, dorsal and ventral finger-vein patterns have indicated a similar performance.

VI. Conclusion

We have developed a new low-cost finger-vein sensor to capture good quality finger-vein images from both ventral and dorsal region in two separate capture processes. The goal of

this work is to explore the effectiveness of the illumination type (side, top and both) and also the type of finger-vein (dorsal/ventral). To this extent, we have presented two new finger-vein databases: DB-I with 350 unique finger-vein instances captured in three different illumination types, DB-II with 1084 unique instances collected using both illuminations. An extensive evaluation is carried out on eight different SOTA methods on two different large-scale databases (DB-I and DB-II). The results indicate the use of Both-light illumination (side + top) to achieve high verification accuracy. This further justifies the design and applicability of the developed sensor in the real-life scenario. The obtained results on DB-II also indicate the applicability of the dorsal finger-vein characteristics for the real-life applications.

ACKNOWLEDGMENT

This work is carried out under the partial funding of the Research Council of Norway (Grant No. IKTPLUSS 248030/O70) and Center for Cyber and Information Security (CCIS), NTNU, Norway.

APPENDIX

In the following Tables V and VI presents the performance of eight different state-of-the-art methods employed in this work on DB-I and DB-II respectively. Since EER is not a recommended metric to evaluate the performance of a biometric systems following the International Standard ISO/IEC 19795-1:2006 on Biometric Performance Testing and Reporting (BPTR) [28], we have included this just for reference and it can be noticed that the EER values are lower with both-light illumination.

REFERENCES

[1] R. Raghavendra and C. Busch, "Presentation attack detection algorithms for finger vein biometrics: A comprehensive study," in *11th International Conference on Signal-Image Technology & Internet-Based Systems (SITIS)*. IEEE, 2015, pp. 628–632.

[2] R. Raghavendra, J. Surbiryala, K. B. Raja, and C. Busch, "Novel finger vascular pattern imaging device for robust biometric verification," in *Imaging Systems and Techniques (IST), 2014 IEEE International Conference on*. IEEE, 2014, pp. 148–152.

[3] A. Kumar and Y. Zhou, "Human identification using finger images," *IEEE Transactions on Image Processing*, vol. 21, no. 4, pp. 2228–2244, 2012.

[4] B. Huang, Y. Dai, R. Li, D. Tang, and W. Li, "Finger-vein authentication based on wide line detector and pattern normalization," in *20th International Conference on Pattern Recognition*, Aug 2010, pp. 1269–1272.

[5] B. Ton and R. Veldhuis, "A high quality finger vascular pattern dataset collected using a custom designed capturing device," in *International Conference on Biometrics (ICB)*, 2013, pp. 1–5.

[6] W. Yang, X. Yu, and Q. Liao, "Personal authentication using finger vein pattern and finger-dorsa texture fusion," in *Proceedings of the 17th ACM International Conference on Multimedia*, ser. MM '09, 2009, pp. 905–908.

[7] X. Xi, G. Yang, Y. Yin, and X. Meng, "Finger vein recognition with personalized feature selection," *Sensors*, vol. 13, no. 9, pp. 11 243–11 259, 2013.

[8] W. Yang, Q. Rao, and Q. Liao, "Personal identification for single sample using finger vein location and direction coding," in *Hand-Based Biometrics (ICHB), 2011 International Conference on*. IEEE, 2011, pp. 1–6.

[9] R. Raghavendra, K. B. raja, J. Surbiryala, and C. Busch, "A low-cost multimodal biometric sensor to capture finger vein and fingerprint," in *International Joint Conference on Biometrics (IJCB)*, Sep 2014, pp. 1–7.

[10] Y. Lu, S. J. Xie, S. Yoon, Z. Wang, and D. S. Park, "An available database for the research of finger vein recognition," in *2013 6th International Congress on Image and Signal Processing (CISP)*, vol. 01, Dec 2013, pp. 410–415.

[11] D. T. N. S. Y. K. Tuyen Danh Pham, Young Ho Park and K. R. Park, "Nonintrusive finger-vein recognition system using nir image sensor and accuracy analyses according to various factors," *Sensor*, vol. 15, no. 7, p. 16866âĂŞ16894, 2015.

[12] Y. Dai, B. Huang, W. Li, and Z. Xu, "A method for capturing the finger-vein image using nonuniform intensity infrared light," in *Congress on Image and Signal Processing*, vol. 4, 2008, pp. 501–505.

[13] M. Kono, H. Ueki, and S.-i. Umemura, "Near-infrared finger vein patterns for personal identification," *Applied Optics*, vol. 41, no. 35, pp. 7429–7436, 2002.

[14] J. Kim, H.-J. Kong, S. Park, S. Noh, S.-R. Lee, T. Kim, and H. C. Kim, "Non-contact finger vein acquisition system using nir laser," in *Sensors, Cameras, and Systems for Industrial/Scientific Applications X*, vol. 7249. International Society for Optics and Photonics, 2009, p. 72490Y.

[15] D. HejtmÃąnkovÃą, R. DvoÅŹÃąk, M. DrahanskÃ¡, and F. OrsÃąg, "A new method of finger veins detection," *International Journal of Bio-Science and Bio-Technology*, vol. 1, no. 1, 2009.

[16] O. Carnal and J. Mlynek, "Young's double-slit experiment with atoms: A simple atom interferometer," *Physical review letters*, 1991.

[17] K. Shaheed, H. Liu, G. Yang, I. Qureshi, J. Gou, and Y. Yin, "A systematic review of finger vein recognition techniques," *Information*, vol. 9, no. 9, 2018. [Online]. Available: http://www.mdpi.com/2078-2489/9/9/213

[18] N. Miura, A. Nagasaka, and T. Miyatake, "Extraction of finger-vein patterns using maximum curvature points in image profiles," *IEICE TRANSACTIONS on Information and Systems*, vol. 90, no. 8, pp. 1185–1194, 2007.

[19] D. Hartung, M. Aastrup Olsen, H. Xu, H. Thanh Nguyen, and C. Busch, "Comprehensive analysis of spectral minutiae for vein pattern recognition," *IET Biometrics*, vol. 1, no. 1, pp. 25–36, March 2012.

[20] N. Miura, A. Nagasaka, and T. Miyatake, "Feature extraction of finger-vein patterns based on repeated line tracking and its application to personal identification," *Machine Vision and Applications*, vol. 15, no. 4, pp. 194–203, 2004.

[21] E. C. Lee, H. Jung, and D. Kim, "New finger biometric method using near infrared imaging," *Sensors*, vol. 11, no. 3, pp. 2319–2333, 2011. [Online]. Available: http://www.mdpi.com/1424-8220/11/3/2319

[22] K. Wang, A. S. Khisa, X. Wu, and Q. Zhao, "Finger vein recognition using lbp variance with global matching," in *International Conference on Wavelet Analysis and Pattern Recognition*, July 2012, pp. 196–201.

[23] J. Yang, Y. Shi, J. Yang, and L. Jiang, "A novel finger-vein recognition method with feature combination," in *2009 16th IEEE International Conference on Image Processing (ICIP)*, Nov 2009, pp. 2709–2712.

[24] Y. Lu, S. Yoon, S. J. Xie, J. Yang, Z. Wang, and D. S. Park, "Finger vein recognition using histogram of competitive gabor responses," in *22nd International Conference on Pattern Recognition*, Aug 2014, pp. 1758–1763.

[25] S. Cai, L. Zhang, W. Zuo, and X. Feng, "A probabilistic collaborative representation based approach for pattern classification," 2016.

[26] K. R. C. B. R. Raghavendra, Sushma Venkatesh, "A low-cost multi-fingervein verification system," in *International Conference on Imaging Systems and Techniques (IST)*, Oct 2018, pp. 1–8.

[27] Y. Fang, Q. Wu, and W. Kang, "A novel finger vein verification system based on two-stream convolutional network learning," *Neurocomputing*, vol. 290, pp. 100 – 107, 2018.

[28] ISO/IEC TC JTC1 SC37 Biometrics, *ISO/IEC 19795-1:2006. Information Technology – Biometric Performance Testing and Reporting – Part 1: Principles and Framework*, International Organization for Standardization and International Electrotechnical Committee, Mar. 2006.

Algorithms		Side illumination		Back illumination		Both illumination	
		EER (%)		EER (%)		EER (%)	
		Dorsal	Ventral	Dorsal	Ventral	Dorsal	Ventral
Global Features	HoG features [24]	0.01	0	0.01	0.01	0	0
	LBP features [21]	4.30	5.59	2.28	4.31	0.92	1.91
	LBPV features [22]	28.30	28.03	22.97	13.25	9.45	12.83
	Steerable features [23]	1.72	1.71	0.05	1.72	0.22	0.22
	CNN [27]	0.21	0.01	0.01	0	0	0
Local features	MCP [18]	4.57	2.28	4.12	0.57	0.28	0.57
	SMR [19]	4.57	2.71	4.28	1.71	0.04	0.49
	RLT [20]	4.97	1.71	4.28	1.71	0.29	0.87

TABLE V: Performance (in EER (%)) of the SOTA finger-vein recognition algorithms on different kind of illuminations

Algorithms		EER(%)	
		Dorsal Fingervein	Ventral Fingervein
Global features	HoG features [24]	0	0.18
	LBP features [21]	4.17	3.54
	LBPV features [22]	4.62	6.55
	Steerable features [23]	3.44	2.97
	CNN [27]	0.08	0.14
Local features	MCP [18]	0.27	0.34
	SMR [19]	0.28	0.22
	RLT [20]	0.65	0.61

TABLE VI: Performance (in EER (%)) of the SOTA finger-vein recognition algorithms on DB-II